

Supporting Information

Intriguing structural transition inducing the variable birefringences in

$\text{ABa}_2\text{MS}_4\text{Cl}$ (A = Rb, Cs; M = Ge, Sn)

Yu Chu,^{a,b} Kui Wu,^{a,*} Xin Su,^a Jian Han,^a Zhihua Yang,^a Shilie Pan^{a,*}

^a*CAS Key Laboratory of Functional Materials and Devices for Special Environments,
Xinjiang Technical Institute of Physics & Chemistry, CAS; Xinjiang Key Laboratory
of Electronic Information Materials and Devices, 40-1 South Beijing Road, Urumqi*

830011, China

^b*University of Chinese Academy of Sciences, Beijing 100049, China*

To whom correspondence should be addressed :

E-mail: slpan@ms.xjb.ac.cn (Shilie Pan).

**E-mail: wukui@ms.xjb.ac.cn (Kui Wu).*

CONTENTS

1. Synthesis of Title Compounds
2. Structural Refinement and Crystal Data
3. Property Characterization
4. Figures and Tables
5. References

1. Synthesis of Title Compounds

All the starting materials were used as purchased without further refinement. In the preparation process, a graphite crucible was added into the vacuum sealed silica tube evacuated to 10^{-3} Pa to avoid the reaction between halides (ACl) and silica tube at the high temperature. α -ABa₂MS₄Cl (A = Rb, Cs; M = Ge, Sn) were prepared with a mixture under an Ar atmosphere in a glovebox at the stoichiometric ratio of ACl: BaS: (Ge or Sn) : S = 1 : 2 : 1 : 2, respectively. The temperature process was set as follows: firstly, the microchip-controlled furnace was heated to 800 °C in 40 h, and kept at this temperature about 3 days, then, slowly down to 300 °C with the ratio of 5 °C/h, eventually, swiftly cooled to room temperature. Obtained products were washed by the N, N-dimethylformamide (DMF) solvent. Near-colorless crystals for α -ABa₂GeS₄Cl and yellow crystals for α -ABa₂SnS₄Cl were found and stable in air. As for β -CsBa₂SnS₄Cl, the initial reagents were the mixture of CsCl, BaS, Sn, and S with the ratio of 1:4:3:6. The temperature process is similar to that of α -form. After washed with the DMF solvent, yellow crystals for β -CsBa₂SnS₄Cl are found, which are also stable in the air for several months. Unfortunately, the α -form often coexists with the β -form and it is difficult to separate them, adjusting the ratio of reactants and the reaction temperature is still difficult to increase the yield of target compound. Consequently, the relative measurements have not been achieved for this compound. A Bruker D2 X-ray diffractometer with Cu K α radiation ($\lambda = 1.5418$ Å) was used to measure the powder X-ray diffraction (XRD) patterns of title grinded compounds at room temperature. The measured range is 10-70° with a step size of 0.02°. Compared with the calculated and experiment results (Figures S1), it is obvious that they are basically consistent with each other.

2. Structural Refinement and Crystal Data

Carefully selected single-crystals were used for data collections with a Bruker SMART APEX II 4K CCD diffractometer using Mo K α radiation ($\lambda = 0.71073$ Å) at room temperature. Multi-scan method was used for absorption correction. All the crystal structures were solved by direct method and refined using the SHELXTL program package.¹ For purpose of structure determination, the semiquantitative

energy dispersive X-ray spectra (EDX) was used to determine the elements of obtained crystals, which includes Rb, Ba, Sn, S, and Cl. The bond-valence method was also used to resolve the structure. Besides, multi-scan method was used for absorption correction. Rational anisotropic thermal parameters for all atoms were obtained by the anisotropic refinement and extinction correction. PLATON was also performed to check the final structure and no other symmetries were found.² Detail refinement parameters and data were shown in Table S1.

3. Property Characterization

UV–Vis–Near-IR (NIR) Diffuse-Reflectance Spectra

Diffuse-reflectance spectra were measured by a Shimadzu SolidSpec-3700DUV spectrophotometer in the wavelength range of 190–2600 nm at room temperature. The absorption spectra were converted from the reflection spectra via the Kubelka–Munk function. IR spectra were collected with a Shimadzu IR Affinity-1 Fourier transform infrared spectrometer in wavenumber range from 400 to 4000 cm^{-1} using picked single-crystals mixed with KBr pellets.

Raman Spectroscopy

Hand-picked crystals were firstly put on an object slide, and then a LABRAM HR Evolution spectrometer equipped with a CCD detector by a 532 nm laser was used to record the Raman spectra. The integration time was set to be 5 s.

Computational Description

Utilized the plane wave pseudopotential method implemented in the CASTEP, the electronic structures of tile compounds were performed on DFT.³ The Perdew-Burke-Ernzerhof (PBE) exchange-correlation of Generalized Gradient Approximation (GGA) was chosen for $\text{CsBa}_2\text{GeS}_4\text{Cl}$, $\text{RbBa}_2\text{GeS}_4\text{Cl}$, and $\beta\text{-CsBa}_2\text{SnS}_4\text{Cl}$, while $\alpha\text{-CsBa}_2\text{SnS}_4\text{Cl}$ and $\text{RbBa}_2\text{SnS}_4\text{Cl}$ were optimized by the local density approximation (LDA) with the Ceperley-Alder exchange-correlation potential as parametrized by Perdew-Zunger (CA-PZ) and at the same time relaxed using the Pulay density-mixing scheme of electronic minimization to increase robustness

instead of the self-consistent minimization of the total energy.⁴

Despite the fact that GGA-PBE method is adequately eligible to describe the electronic structures and optical properties in terms of numerous crystals, the LDA-CA-PZ-calculated band gaps of α -CsBa₂SnS₄Cl and RbBa₂SnS₄Cl is in better agreement with the experiments instead of PBE. Optimized norm-conserving pseudopotential (NCP) in the Kleinman–Bylander form was employed and the valance electrons of the related atoms were: Rb 4s² 4p⁶ 5s¹, Cs 5s² 5p⁶ 6s¹, Ba 5s² 5p⁶ 6s², Ge 4s² 4p², Sn 5s² 5p², S 3s² 3p⁴, and Cl 3s² 3p⁵, respectively.⁵ Also, kinetic energy cut-offs was set to be 750.0 eV and Monkhorst-Pack *k*-point meshes ($3 \times 3 \times 2$) with a density of 0.04 Å⁻¹ in the Brillouin zone (BZ) was adopted.⁶

Since α -ABa₂MS₄Cl crystallizes in the monoclinic space group, which pertains to biaxial crystal, geometrical optimizations were deployed for calculating polarizability in order to determine the directions of two different optic axes wherein these structures were relaxed using the Broyden-Fletcher-Goldfarb-Shanno (BFGS) method. In addition, the all Bands/EDFT electronic minimizer rather than density mixing minimizer was used for the sake of efficiency.

Other important optical parameters such as reflective index and birefringence, were calculated with the scissors operators revised.⁷⁻⁹ It is proverbial that the refractive indices are obtained theoretically from the imaginary part of the dielectric function through the Kramers-Kroning transform. The imaginary part can be calculated with the matrix elements that describe the electronic transitions in the considered crystals. To further investigate the influence of the cation and anionic groups on the optical response of ABa₂MS₄Cl, and the differentiability caused by phase-transformation, a real-space atom-cutting method was used.

In previous research¹⁰ we found that the charge density around Cs, Ba and Cl is spherical, so we first chose the cutting radius of Cs, Ba and Cl to be 1.70, 1.37 and 1.83 Å. Besides, following the rule of keeping the cutting spheres of the cation or anionic group in contact and not overlapped, the cutting radius of S is set to be 1.24 Å. Finally, the covalent radius 1.55 Å of Sn is chosen as its cutting radius in order to totally separate the electronic cloud density of the SnS₄ group.

4. Figures and Tables

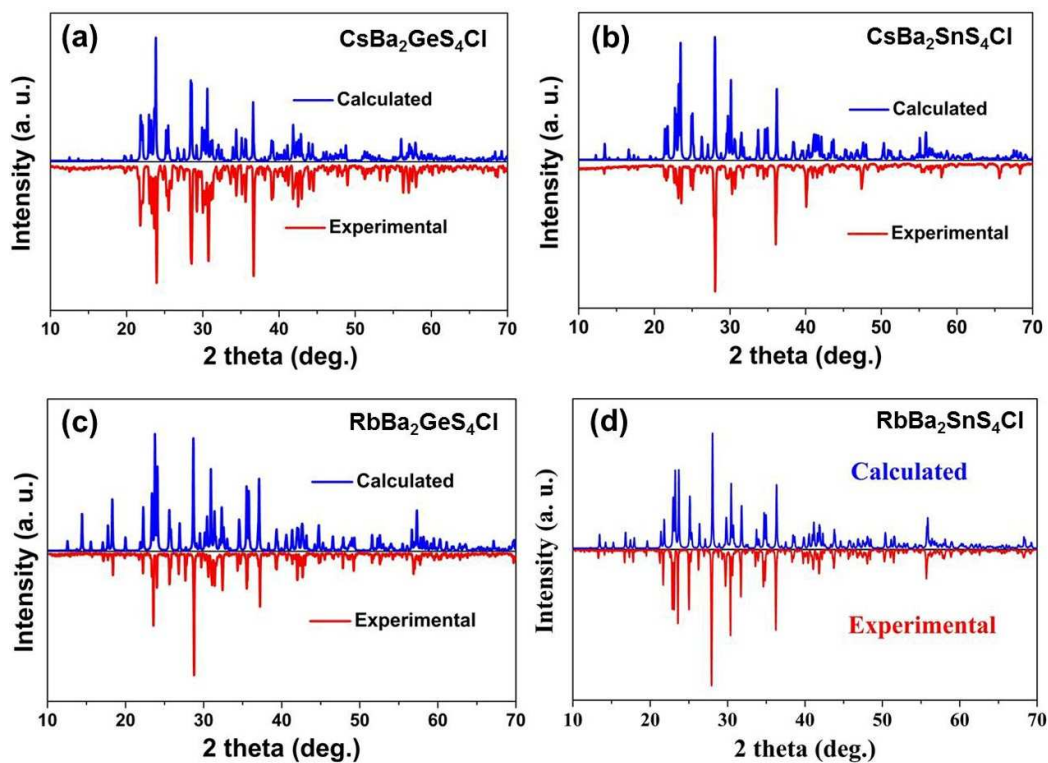


Figure S1. Experimental and calculated powder X-ray diffraction data.

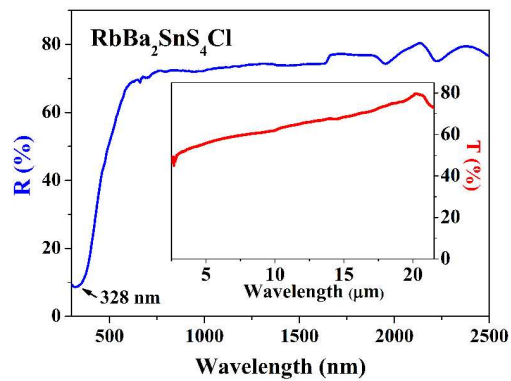


Figure S2. Diffuse-reflection spectrum of $\text{RbBa}_2\text{SnS}_4\text{Cl}$.

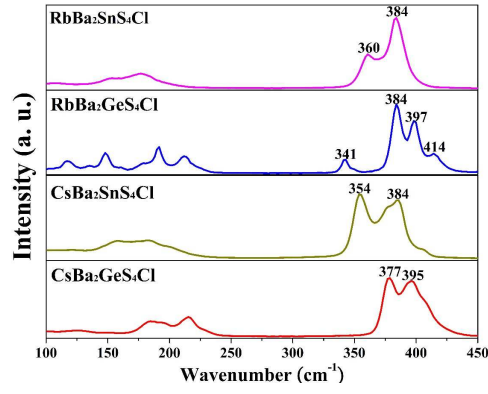


Figure S3. Raman spectra of α -ABa₂MS₄Cl (A = Rb, Cs; M = Ge, Sn).

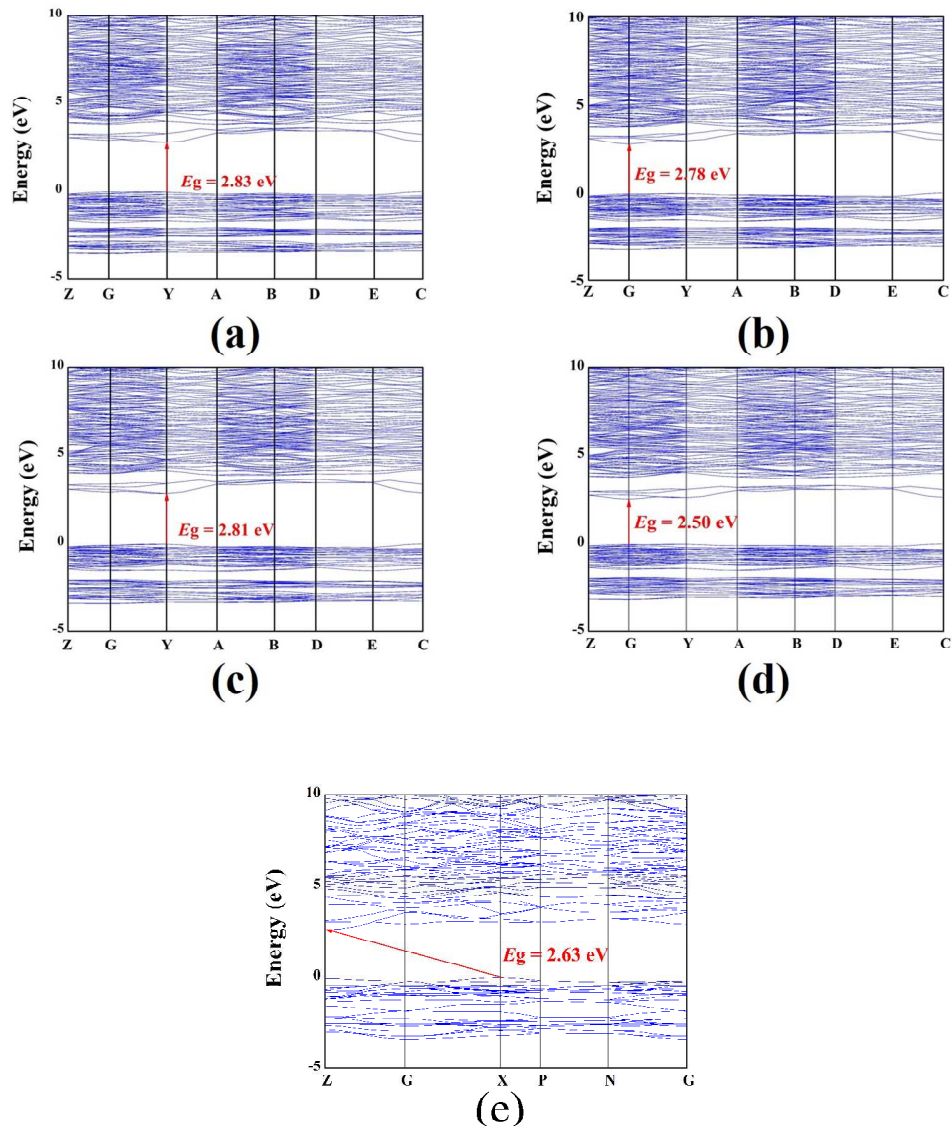


Figure S4. Band structures of RbBa₂GeS₄Cl (a), RbBa₂SnS₄Cl (b), CsBa₂GeS₄Cl (c), α -CsBa₂SnS₄Cl (d), and β -CsBa₂SnS₄Cl (e).

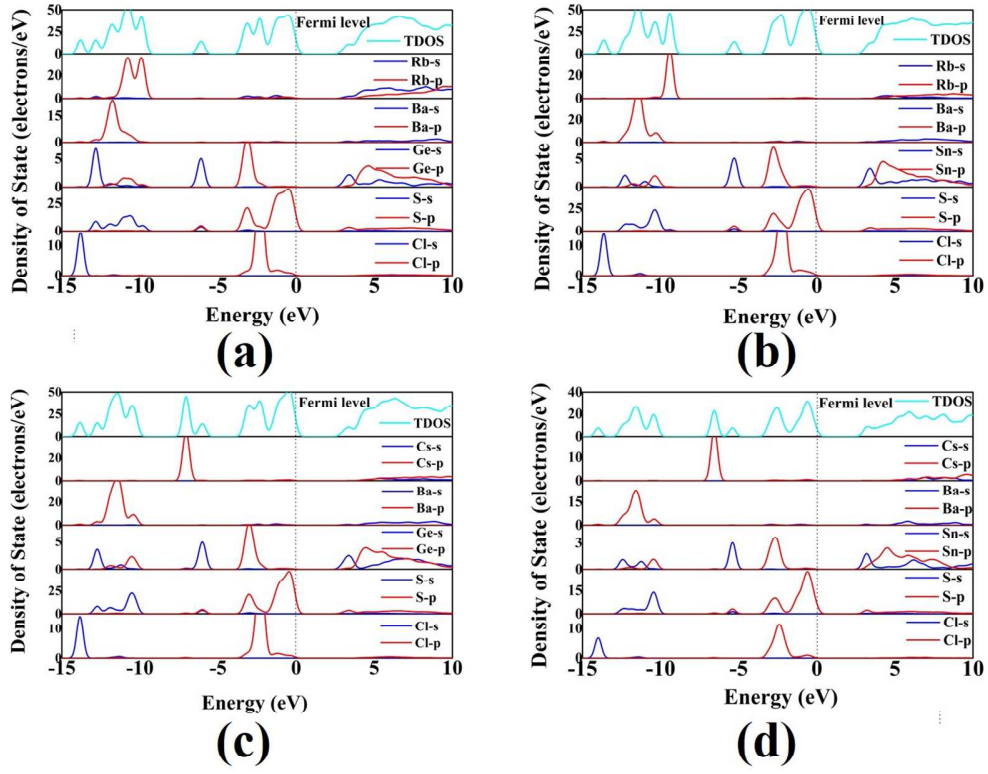


Figure S5. PDOS and TDOS plots of $\text{RbBa}_2\text{GeS}_4\text{Cl}$ (a), $\text{RbBa}_2\text{SnS}_4\text{Cl}$ (b), $\text{CsBa}_2\text{GeS}_4\text{Cl}$ (c), and $\beta\text{-CsBa}_2\text{SnS}_4\text{Cl}$ (d).

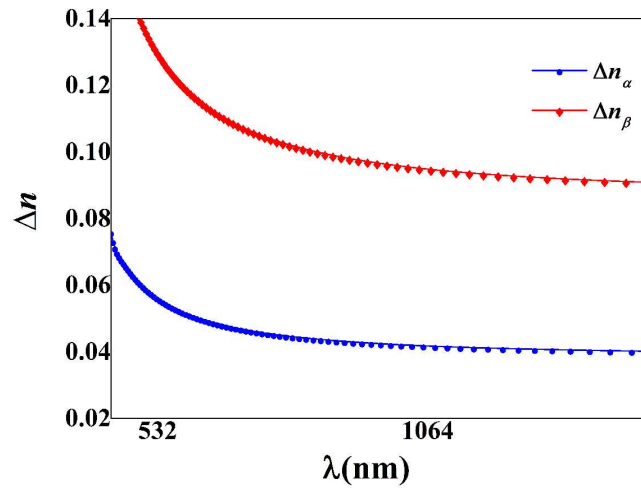


Figure S6. Dispersion of birefringence Δn of $\alpha\text{-CsBa}_2\text{SnS}_4\text{Cl}$, and $\beta\text{-CsBa}_2\text{SnS}_4\text{Cl}$

Table S1 (a) Crystal data and structure refinement for RbBa₂GeS₄Cl, RbBa₂SnS₄Cl
and CsBa₂GeS₄Cl.

Empirical formula	CsBa ₂ GeS ₄ Cl	RbBa ₂ GeS ₄ Cl	RbBa ₂ SnS ₄ Cl
Formula weight	643.87	596.43	642.53
Temperature	296 (2) K	296 (2) K	296 (2) K
Crystal system	<i>Monoclinic</i>	<i>Monoclinic</i>	<i>Monoclinic</i>
Space group	<i>P2₁/c</i>	<i>P2₁/c</i>	<i>P2₁/c</i>
Unit cell dimensions	a = 9.8126(17) Å	a = 9.6857(13) Å	a = 9.883(6) Å
	b = 8.6107(13) Å	b = 8.5955(13) Å	b = 8.806(5) Å
	c = 12.416(2) Å	c = 12.269(18) Å	c = 12.437(7) Å
	β = 90.738(12)	β = 90.118(8)	β = 90.144(7)
Z, V	4, 1049.0(3) Å ³	4, 1021.4(3) Å ³	4, 1082.4(11) Å ³
Density (calculated)	4.077 g/cm ³	3.878 g/cm ³	3.943 g/cm ³
Completeness to theta = 27.50	99.1%	99.7%	99.7%
Goodness-of-fit on <i>F</i> ²	0.995	1.109	1.002
Final <i>R</i> indices	<i>R</i> ₁ = 0.0491	<i>R</i> ₁ = 0.0380	<i>R</i> ₁ = 0.0372
[<i>F</i> _o ² > 2σ(<i>F</i> _o ²)] ^[a]	<i>wR</i> ₂ = 0.1183	<i>wR</i> ₂ = 0.0930	<i>wR</i> ₂ = 0.0732
R indices (all data) ^[a]	<i>R</i> ₁ = 0.0918 <i>wR</i> ₂ = 0.1561	<i>R</i> ₁ = 0.0464 <i>wR</i> ₂ = 0.0969	<i>R</i> ₁ = 0.0523 <i>wR</i> ₂ = 0.0787
Largest diff. peak and hole (e Å ⁻³)	2.482, -2.712	2.532, -1.537	1.455, -1.182

Table S1 (b) Crystal data and structure refinement for α -CsBa₂SnS₄Cl and β -CsBa₂SnS₄Cl.

Empirical formula	α -CsBa ₂ SnS ₄ Cl	β -CsBa ₂ SnS ₄ Cl
Formula weight	689.97	689.97
Temperature	296 (2) K	296(2) K
Crystal system	<i>Monoclinic</i>	<i>Tetragonal</i>
Space group	<i>P2₁/c</i>	<i>I4/mcm</i>
Unit cell dimensions	a = 9.924(3) Å b = 8.790(3) Å c = 12.598(4) Å β = 90.35(2)	a = 8.487(3) Å c = 14.335(9) Å
Z, V	4, 1098.9(6) Å ³	4, 1032.5(10) Å ³
Density (calculated)	4.170 g/cm ³	4.438 g/cm ³
Completeness to theta = 27.50	100.0%	100%
Goodness-of-fit on F^2	1.077	1.113
Final R indices [$F_o^2 > 2\sigma(F_o^2)$] ^[a]	$R_1 = 0.0359$ $wR_2 = 0.0898$	$R_1 = 0.0341$ $wR_2 = 0.0971$
R indices (all data) ^[a]	$R_1 = 0.0455$ $wR_2 = 0.0942$	$R_1 = 0.0366$ $wR_2 = 0.1001$
Largest diff. peak and hole (e Å ⁻³)	2.173, -2.310	2.597, -1.801

Table S2 Mulliken atomic populations of CsBa₂GeS₄Cl

Charge Q (in e)					
Atom	Cs	Ba	Ge	S	Cl
population	0.92	0.95– 0.96	0.52	0.65 – 0.73	0.57

Table S3 Bond distances and Mulliken overlap populations for characteristic atomic pairs in CsBa₂GeS₄Cl.

Value Atomic/ pair	bond distances/ d (Å)	overlap populations/(e)
Ge-S	2.2010(0) – 2.2348(4)	0.64 – 0.81
Cs-S	3.4504(4) – 3.5956(9)	0-0.02
Cs-Cl	3.5935(8)	0.05
Ba-S	3.1663(1) – 3.3723(0)	0.11 – 0.17
Ba-Cl	3.2014(1) - 3.5922(4)	0.05 - 0.12

Table S4 theoretical and experimental optical properties of title compounds

Compound	Band gap(eV) (Cal.)	Band gap(eV) (Exp.)	Birefringence @1064 nm
RbBa ₂ GeS ₄ Cl	2.83	3.43	0.03
RbBa ₂ SnS ₄ Cl	2.78	2.82	0.031
CsBa ₂ GeS ₄ Cl	2.81	3.33	—
α -CsBa ₂ SnS ₄ Cl	2.50	2.60	0.033
β -CsBa ₂ SnS ₄ Cl	2.63	—	0.094

Table S5. Comparison of the refractive indices of α - and β -CsBa₂SnS₄Cl at the static limit derived from cut- M (M =Cl, Cs, Ba) functions and (SnS₄)⁴⁻ cut wave functions with original values.

Compound		n_x	n_y	n_z	$\Delta n(n_{max}-n_{min})^a$
α -CsBa ₂ SnS ₄ Cl	Total	2.278	2.319	2.310	0.041
	Cs cut	2.209	2.252	2.251	0.043
	Ba cut	2.175	2.205	2.199	0.030
	(SnS ₄) ⁴⁻ cut	1.622	1.631	1.624	0.007
	Cl cut	2.179	2.227	2.217	0.048
Compound		n_o^b	n_e^c	$\Delta n(n_o-n_e)$	
β -CsBa ₂ SnS ₄ Cl	Total	2.212	2.307	0.095	
	Cs cut	2.192	2.289	0.097	
	Ba cut	2.115	2.218	0.103	
	(SnS ₄) ⁴⁻ cut	1.769	1.774	0.005	
	Cl cut	2.132	2.249	0.117	

^a n_{max} is the maximal value of the refractive indices and n_{min} is the minimal value of the refractive indices.

^b n_o is the refractive index of ordinary light in crystal.

^c n_e is the refractive index of extraordinary light in crystal.

5. References

- 1 Sheldrick, G. M. *SHELXTL*, version 6.14, Bruker Analytical X-ray Instruments, Inc. Madison, WI, 2008.
- 2 Spek, A. L. Single-crystal structure validation with the program PLATON. *J. Appl. Crystallogr.* **2003**, *36*, 7.
- 3 Clark, S. J.; Segall, M. D.; Pickard, C. J.; Hasnip, P. J.; Probert, M. J.; Refson, K.; Payne, M. C. First principles methods using CASTEP. *Z. Kristallogr.* **2005**, *220*,

567.

- 4 Kohn, W.; Sham, L. Self-consistent equations including exchange and correlation effects. *J. Phys. Rev.* **1965**, *140*, 1133.
- 5 Perdew, J. P.; Burke, K.; Ernzerhof, M. Generalized gradient approximation made simple. *Phys. Rev. Lett.* **1996**, *77*, 3865.
- 6 Monkhorst, H. J.; Pack, J. D. Special points for Brillouin-zone integrations. *Phys. Rev. B* **1976**, *13*, 5188.
- 7 Chen, C. T.; Lin, Z. S.; Wang, Z. Z. The development of new borate-based UV nonlinear optical crystals. *Appl. Phys. B: Laser Opt.* **2005**, *80*, 1.
- 8 Godby, R. W.; Schluter, M.; Sham, L. Self-energy operators and exchange-correlation potentials in semiconductors. *J. Phys. Rev. B* **1988**, *37*, 10159.
- 9 Wang, C. S.; Klein, B. M. First-principles electronic structure of Si, Ge, GaP, GaAs, ZnS, and ZnSe. II. Optical properties. *Phys. Rev. B* **1981**, *24*, 3417.
- 10 Lin, J.; Lee, M. H.; Liu, Z. P.; Chen, C. T.; Pickard, C. J. Mechanism for linear and nonlinear optical effects in β -BaB₂O₄ crystals. *Phys. Rev. B* **1999**, *60*, 13380.